HHS Public Access

Author manuscript

Nat Neurosci. Author manuscript; available in PMC 2017 March 01.

Published in final edited form as:

Nat Neurosci. 2016 September ; 19(9): 1197–1200. doi:10.1038/nn.4357.

Diminished KCC2 confounds synapse-specificity of LTP during senescence

Isabella Ferando[1], **Guido Faas**[1], and **Istvan Mody**[1,2]

[1]Departments of Neurology, The David Geffen School of Medicine, University of California, Los Angeles, CA, USA

[2]Physiology, The David Geffen School of Medicine, University of California, Los Angeles, CA, USA

Abstract

Synapse-specificity of LTP ensures that no interference arises from inputs irrelevant to the memory to be encoded. In hippocampi of aged (21-28 months-old) mice LTP was relayed to unstimulated synapses blemishing its synapse-specificity. Diminished levels of the K^+/Cl^- cotransporter KCC2 and a depolarizing $GABA_A$ receptor-mediated synaptic component following LTP were the most likely causes for spreading the potentiation, unveiling novel mechanisms hindering information storage in the aged brain, and identifying KCC2 as a potential target for intervention.

Aging is associated with decreased learning and memory even in the absence of Alzheimer's disease[1]. The cellular substrates of this cognitive decline are poorly understood, but may relate to altered long-term potentiation (LTP)[2], regarded as a key mechanism underlying information storage[3]. A hallmark of LTP is its dendritic clustering[4] providing specific potentiation to synapses activated by a high-frequency stimulus. Currently, LTP is considered a “clustered plasticity” confined to specific dendritic domains where spines or small dendritic areas with diffusional links[4] represent computational memory storage units. Spread of plasticity to elements not part of the memory-related cluster interferes with the learning and memory process[5]. Synaptic specificity of LTP reportedly breaks down with age[1,2,6,7]. Here we address potential mechanisms underlying this memory interference at an advanced age in mice.

In slices prepared from 3.75 to 6.25-month-old mice (“young”) and 21 to 28-month-old mice (“old”) we recorded evoked field responses (fEPSPs) from two isolated synaptic inputs (Supplementary Fig. 1) in area CA1 of the hippocampus. These mouse ages correspond to

Correspondence should be directed to Prof. Istvan Mody, Ph.D., Department of Neurology, NRB1 Room 575D, The David Geffen School of Medicine at UCLA, 635 Charles Young Drive South, Los Angeles, CA 90095-733522, Tel: (310)-206-4481, Fax: (310)-825-0033, mody@ucla.edu.

Author Contributions: IF performed experiments and collected data. IF, GF and IM conceived the study, designed experiments, analyzed and interpreted data, prepared figures, and wrote manuscript.

Competing Financial Interests: The authors declare no competing financial interests.

20-26 years and 61.4-78.2 years, respectively, in humans (Supplementary Fig.2). LTP was induced by theta-burst stimulation[8] (TBS). As previously reported in 12 to 14-month-old mice[6,7] (~40-45 years in humans), LTP showed no synapse specificity (Fig.1a; Supplementary Table1). These data are a subset of all LTP experiments (n=17 young and n=21 old mice) where the magnitude of LTP in old, 40 min after TBS, was larger than in young (fEPSP slope as ratio to pre-TBS values, old: 2.23±0.16, n=44 slices, young: 1.67±0.07, n=37 slices, p=0.0022, t=3.321, df=58.5, two-tailed unpaired t-test, unequal variances) mostly due to a larger proportion of rising LTP and some very large magnitude LTP in the old (Supplementary Fig.3). Paired-pulse facilitation (PPF) of fEPSPs was similar in young and old, but a small decrease in PPF was detected after potentiation of the untetanized pathway in old (Supplementary Fig.4). Thus, memory impairments during senescence do not necessarily result from deficits in LTP induction or its decreased magnitude[9], but possibly from the spread of potentiation to unstimulated synapses.

Glutamatergic synapses outnumber GABAergic ones in the apical dendrites of CA1 pyramidal cells[10], but when the $GABA_A$ receptors' reversal potential (E_{GABA}) is sufficiently negative, the latter synapses can reduce both dendritic Ca^{2+} spiking/signaling[11] and LTP[12]. The competitive $GABA_A$ receptor antagonist gabazine (GBZ 25μM) marginally enhanced LTP in young, but surprisingly, blocked LTP induction and its spread to unstimulated synapses in old (Fig.1b). L-655,708 (200nM), a negative allosteric modulator of α5 subunit-containing $GABA_A$ receptors, also partially antagonized LTP in old (Supplementary Fig.5a). Blocking NMDA receptors critical for LTP induction[3] (D-AP5 50μM) fully blocked LTP in young, but only partially in old (Supplementary Fig.5b), consistent with the idea of a Ca^{2+} dysregulation contributing to LTP induction observed in 12 months-old mice[6,7]. Applying GBZ *before* (Supplementary Fig.6a) and 40 min *after* (Supplementary Fig.6b) LTP induction reduced fEPSPs only in old and only in the tetanized input. To further probe the participation of $GABA_A$ receptors in fEPSPS we applied the antagonist bicucculine methiodide (BMI) by rapid iontophoresis in the stratum radiatum. In young, BMI iontophoresis had no effect on fEPSPs before or after LTP induction. In sharp contrast, BMI reversibly reduced fEPSPs when applied after LTP induction in old, even as early as 12-14 min after TBS (Fig.1c&d; Supplemetary Table2). Thus far, our results are consistent with a depolarizing $GABA_A$ receptor-mediated component contributing to the induction (Fig.1b) and maintenance (Fig. 1c&d) of LTP, and potentially, even to the spread of LTP to unstimulated synapses in old. A depolarizing dendritic GABA response had to arise during or immediately after the TBS, as BMI iontophoresis (Fig.1e) or gabazine perfusion did not affect dendritic fEPSPs recorded before TBS in old (Supplementary Fig.6a). Accordingly, LTP in untetanized synapses could ensue through a depolarizing GABA response during TBS that is no longer present 40 min later (Supplementary Fig.6b).

Phasic and tonic GABAergic events in CA1 pyramidal cells in whole-cell recordings showed no differences between young and old (Supplementary Fig.7). We next used pharmacological and optogenetic means to alter Cl^- in CA1 pyramidal cell dendrites. Preincubation of young with the KCC2 antagonist VU0240551[13-15] (for 1 hr, 10 μM) enhanced LTP and spread the potentiation to unstimulated synapses (Fig.2a&b), resembling untreated old. Conversely, the KCC2 enhancer CLP257[13] (1 hr preincubation, 100 μM) had little effect on LTP in old, but more importantly, confined the potentiation solely to the

tetanized synapses (Fig.2a&b). Thus, in the old CLP257 restored properties of LTP to those seen in young, indicating that KCC2 function might be impaired in senescence. CLP257 in young and VU0240551 in old (Fig.2a&b) were ineffective (Supplemetary Table3). LTP magnitude in the tetanized pathway was uncorrelated with the potentiation of the non-tetanized pathway; therefore, increased LTP by VU0240551 in young or reduced LTP by CLP257 in old were not responsible for changes seen in untetanized pathways (Fig 2c). Quantitative Western blots in young and old CA1 mini slices harvested before, and at two time points (10 min and 40 min) after LTP induction showed significantly reduced levels of monomeric KCC2 in old at both time points after induction of LTP (Fig.3a&b). As KCC2 oligomerization can enhance its function[15], we examined oligomerized KCC2 levels in old and found them to be reduced at 40 min but not at 10 min (Fig.3c&d), producing a lower ratio of mono- to oligomeric KCC2 of at 10 min (0.07±0.02, n=7) than at 40 min (0.16 ±0.04, n=15). We also used another approach to elevate intracellular Cl^- yielding a depolarizing E_{GABA}, i.e., through prolonged activation of the Cl^- pump halorhodopsin (eNpHR3.0), known to produce excessive Cl^- loading of neurons[16]. In slices from young mice expressing eNpHR3.0 in CA1 pyramidal cells (Supplementary Fig.8a&b) 568-nm laser illumination (> 10 min before and during TBS) resulted in very large LTP (Supplementary Fig.8c), resembling those found in the outliers of old (Supplementary Fig.3c). Like in old controls, robust potentiation of the unstimulated pathway ensued in Cl^--loaded young pyramidal cells.

We presented evidence for diminished KCC2 levels after LTP in old, and obtained several signs for altered E_{GABA}: 1) GBZ antagonized LTP induction in old, but had little effect in young; 2) GBZ reduced potentiated responses (after LTP) in old but not in young; 3) after LTP rapid BMI iontophoresis transiently reduced fEPSPs only in old, revealing a depolarizing component; 4) blocking KCC2 in young lead to the loss of its synapse specificity, resembling the old; 5) enhancing KCC2 in old restored the synapse specificity of LTP, as seen in the young; 6) artificial Cl^- loading in young resembled LTP in the old, including loss of synaptic specificity. Yet, none of our approaches directly measured local $\bar{Cl}$ changes in small dendritic compartments or even spines. Somatic recordings only account for the activity of GABAergic synapses close to the cell body[17], whereas E_{GABA} may quickly and dynamically change in a small dendritic volume[18], and may be confined to the spines[19]. Local dendritic alterations in E_{GABA} are impossible to detect with somatic perforated patch recordings or even with the continuously improving Cl^- indicators that are still not without problems[20]. As KCC2 is subject to complex regulatory events including phosphorylation, internalization, and Ca^{2+}-dependent degradation[14,15], the precise mechanisms underlying its failure during repetitive synaptic activation in the aged brain remain to be determined. Pending further verification, we propose that the resulting GABAergic depolarization spreads the Ca^{2+} signal to dendritic branches not destined to be part of clustered plasticity (Supplementary Fig.9). Consequently, plasticity disperses to synapses not involved in transmitting information intended for storage, severely confounding memory induction and retrieval[5]. Conversion of GABAergic inhibition into excitation during repetitive activation of old synapses could also explain why reducing excitability improves cognition in aged humans[21] and rodents[22] alike. Reversal of the blemishing spread of synaptic plasticity in the old brain by a KCC2 enhancer may add the treatment of cognitive

disorders during senescence to the already wide-ranging and promising prospects of clinical applications for such drugs[13].

Online Methods

Animal Subjects

In this study we used young (3.75 to 6.25 months-old, n=45) or old (21-28 months-old, n=35) C57BL/6J mice of both sexes (69 males and 11 females) bred in-house or acquired from the National Institute of Aging (NIA). Halorhodopsin (eNpHR3.0) expressing mice (n=6) were generated by crossing Camk2a-Cre/ERT2 mice (JAX Stock # 012362) with Rosa-CAG-LSL-eNpHR3.0-EYFP-WPRE Ai39 mice (JAX Stock # 014539). Mice were group-housed with *ad libitum* access to food and water on a 12-h light/dark cycle, under the care of the UCLA Division of Laboratory Animal Medicine (DLAM). All experiments were performed according to a protocol (ARC # 1995-045-53B) approved by the UCLA Chancellor's Animal Research Committee. Genotyping was performed by Transnetyx (Memphis, TN, USA).

Slice Preparation and Electrophysiology

Hippocampal slices were prepared as previously reported[23]. Briefly mice were anesthetized with isoflurane and decapitated following UCLA Chancellor's Animal Research Committee protocol. Coronal 350μm slices were cut on a Leica VT1000S vibratome in ice-cold N-Methyl-D-Glucamine (NMDG)-based HEPES-buffered solution, containing in mM: 135 NMDG, 10 D-glucose, 4 $MgCl_2$, 0.5 $CaCl_2$, 1 KCl, 1.2 KH_2PO_4, 20 HEPES, 27 sucrose (bubbled with 100% O_2, pH 7.4, 290 –300 mOsm/L). Slices were incubated at 32°C in an interface chamber in a reduced sodium artificial CSF (aCSF), containing in mM: NaCl 85, D-glucose 25, sucrose 55, KCl 2.5, NaH_2PO_4 1.25, $CaCl_2$ 0.5, $MgCl_2$ 4, $NaHCO_3$ 26, pH 7.3–7.4 when bubbled with 95% O_2, 5% CO_2. After 20 min low sodium aCSF was substituted for normal aCSF (naCSF) at room temperature, containing in mM: NaCl 126, D-glucose 10, $MgCl_2$ 2, $CaCl_2$ 2, KCl 2.5, NaH_2PO_4 1.25, Na Pyruvate 1.5, L-Glutamine 1, $NaHCO_3$ 26, pH 7.3-7.4 when bubbled with 95% O_2, 5% CO_2. Recordings were done in an interface chamber at 35°C perfused with naCSF.

The Schaffer collateral pathway was stimulated every 30 s with two pulses, 50 ms apart. Average stimulus durations (in μs, young: 55.16±0.96, n=116; old: 56.02±1.38, n=96, p=0.6039, t=0.512, df=175.3, two-tailed unpaired t-test), stimulus intensities (in μA, young: 58.49±1.01, n=116; old: 60.77±1.47, n=96, p=0.1925, t=1.308, df=173.9, two-tailed unpaired t-test), and stimulus charges (in nC, young: 3.27±0.10, n=116; old: 3.52±0.16, n=96, p=0.1747, t=1.363, df=163.15, two-tailed unpaired t-test) used in our experiments were all comparable between the two preparations. Similarly, the slopes of the fEPSPs elicited during the control period in the two preparations by the S1 or S2 stimuli were comparable (in V/s, S1 young: 0.543±0.035, n=37; S1 old: 0.594±0.037, n=44, p=0.32, t=1.001, t=78.9, two-tailed unpaired t-test; S2 young: 0.381±0.060, n=8; S2 old: 0.503±0.059, n=15, p=0.20, t=1.33, df=18.46, two-tailed unpaired t-test). Long term potentiation was induced by stimulating the Schaffer collaterals with two-times the duration of baseline stimuli with a theta burst protocol (TBS) repeated twice, 30 s apart (4 pulses, 100

s^{-1} repeated 20 times every 350 ms). Synaptic specificity of the LTP was tested after determining the independence of the two stimulated Schaffer collateral pathways by lack of reciprocal paired pulse interactions. In each of the experiments testing synaptic specificity, one of the two independent pathways was randomly (coin flip) chosen to be tetanized. Evoked fEPSPs were recorded in CA1 stratum radiatum (SR) with the use of a patch pipette (3-5 MΩ resistance) filled with naCSF connected to the headstage of an amplifier (A-M Systems Inc., model 3000) where it was band-pass filtered between 0.1 and 1000 Hz. The signal was fed through an instrumentation amplifier (Brownlee BP Precision, model 210A) and sampled at 10,000 s^{-1} with a National Instruments A/D board. Field potentials were recorded using EVAN (custom-designed LabView-based software from Thotec) and analyzed with a custom written procedure (Wavemetrics, IGOR Pro 6.22A). The slope of the fEPSPs was measured during a 0.5 – 1.0 ms window of their steepest rising phase. The LTP induction was categorized as follows: 1) “no LTP”, when the average of the fEPSP slope measured between 35 and 40 min post-TBS was not significantly ($p<0.05$, Mann-Whitney U-test) larger (i.e., it was equal or smaller) than the average fEPSP slope measured for 5 min just before TBS; 2) “rising LTP”, if the average fEPSP slope measured between 35 and 40 min post-TBS was significantly ($p<0.05$, Mann-Whitney U-test) larger than that measured during the 5 min before TBS, and the fEPSP slope significantly grew over the 20–40 min after the TBS (fEPSP slope vs time, linear regression coefficient > 0, $p<0.05$); 3) “steady state LTP”, if the average fEPSP slope between 35 and 40 min post-TBS was significantly ($p<0.05$, Mann-Whitney U-test) larger than control, but the fEPSP slope did not significantly grow over 20–40 min after TBS (fEPSP slope vs time, linear regression coefficient not significantly ≠ 0, $p>0.05$).

All CA1 pyramidal cell somatic whole-cell recordings were made in naCSF in visually identified neurons (custom-made IR-DIC video-microscopy; Olympus 40× water immersion objective) with an Axopatch 200B amplifier. Recording electrodes were pulled from borosilicate glass capillaries with an inner filament (KG-33, 1.12 mm inner diameter, 1.5 mm outer diameter; Garner Glass) pulled to tip diameters of ~1.0 μm in two stages using a horizontal puller (DMZ Universal Puller, Zeitz Instruments GmbH, Munich, Germany). Intracellular solutions contained the following (in mM): 130 Cs-methylsulphate, 5 CsCl, 10 HEPES, 10 EGTA, 5 MgATP, adjusted to pH 7.25 with CsOH (280-290 mOsm). Voltage-clamp recordings were made at V_h = 0 to +5 mV. The DC resistances of the electrodes were 4 - 6 MW. Series resistance was compensated by 70-90% using lag values of 7-10 μs. Before compensation, series resistance was <15 MΩ.

All drugs were purchased from Tocris. L655,708 (200 nM), D-AP5 (25 μM), SR-95531 hydrobromide (gabazine, abbreviated as GBZ, 20 μM) were perfused either 10 min before or 40 min after TBS. In all experiments where GBZ was perfused, the CA3 was mechanically disconnected from CA1 immediately after slices were prepared, in order to prevent development of spontaneous epileptiform activity in the slices. For VU0240551 (10 μM, previously dissolved in DMSO, final vehicle concentration 0.01%) and CLP257 (100 μM, previously dissolved in DMSO, final vehicle concentration 0.1%) slices were incubated in the drug for 1 h, recordings were done in the continued presence of VU0240551 or in aCSF for slices preincubated in CLP257.

For iontophoresis experiments (-)-bicuculline methiodide (BMI, 10 mM) was dissolved in a 1.5 M NaCl solution, pH 3, and applied through a patch pipette. Typically, ten 50 nA pulses of 300 ms duration were applied to eject BMI with the use of an ultrafast iontophoresis system (MVCS-02C npi, npi electronic GmbH, Germany). Between applications BMI was restricted using an active holding current.

For eNpHR3.0 light stimulation experiments an Ar-Kr laser was used (Cambridge Laser laboratories, Fremont, California). Wavelength selection was done with an AOTF (NEOS) at 568 nm. Light was coupled into an optical fiber (Ø 800 μm) and the total light power used was 5 mW over a tissue area of Ø 1 mm (0.785 mm^2). When used, light was kept on throughout the duration of the experiments.

Quantitative Western Blots

The hippocampal CA area straddling the recording electrode was microdissected from coronal slices immediately after recording and frozen in liquid nitrogen. Control non-LTP slices were kept under the same conditions of perfusion and temperature as slices that received the tetanus. Protein extraction and Western blots were done as previously reported[24]. Briefly, samples were homogenized for 2 minutes in ice-cold homogenization buffer containing in mM: 10 $NaPO_4$, 100 NaCl, 10 $Na_4P_2O_7$, 25 NaF, 5 EDTA, 5 EGTA, 1 Na_3VO_4, 2% Triton X-100, 0.5% deoxycholate, pH 7.4, in the presence of protease inhibitors (for 10 ml, 1 Complete Mini tablet, Roche, and phenylmethanesulfonyl fluoride 100 μM, Sigma). Supernatant was collected after 30 min incubation on ice, and following 20 min centrifugation at 12000 rpm at room temperature. Protein concentrations were determined with *DC*™ Protein Assay (Bio-Rad). Three μg of total protein were diluted in phosphate buffer saline and Laemmli Sample Buffer (Bio-Rad) containing 5% 2-mercaptoethanol (Sigma), and later separated by gel electrophoresis (10% precast polyacrylamide gel, Bio-Rad). Proteins were then transferred to a 0.2 μm PVDF membrane (Bio-Rad). Membranes were blocked in 5% nonfat milk and 2% BSA and blotted in rabbit polyclonal anti-KCC2, 1:1000 (Millipore, 07-432). GAPDH was used as loading control (rabbit monoclonal anti-GAPDH 1:2000, Abcam, ab181602). Membranes were then incubated in anti-rabbit horseradish peroxidase-labeled antibody, 1:2000 (GE Healthcare Lifesciences), and developed with Clarity Western ECL Substrate (Bio-Rad). Chemiluminescence was detected with CL-Xposure films (Thermo-Scientific). Optical density of bands was measured with ImageJ software (NIH). The potentiation measured in the old slices harvested for Western blots at 10 min after TBS (1.66+0.70, n=7) was similar (p=0.21, two-tailed unpaired t-test) to that seen in other old slices at 10 min after TBS (1.86+0.06, n=44).

Immunohistochemistry and Microscopy

Brains were perfused and tissues processed as previously described[23,25]. Briefly, deeply anesthetized mice were transcardially perfused with 50 ml of 4% paraformaldehyde in 0.12 M phosphate buffer, pH 7.3. Brains were cryoprotected in 30% sucrose solution in Millonigs modified PBS, frozen and sectioned (coronal, 35 μm). Slices were mounted and coverslipped. Images were collected using a confocal microscope (Leica TCS SP2) using LAS AF software (Leica Microsystems). Digital projection images of 5 μm z-stacks were

assembled and using NIH ImageJ software. Epifluorescent images were collected using an Olympus BX51 microscope equipped with a Q Imaging Retiga 2000R camera and software. Tiles were captured under the same light intensity and exposure limits and later composed in single images using a Stitching Plugin[26] for ImageJ.

Statistics

No statistical methods were used to pre-determine sample sizes but our sample sizes are similar to or larger than those generally employed in the field. On a daily basis, animals were randomly picked from their home cages by an independent animal technician, and were assigned to the various experimental procedures by the experimenter. Collection of data was not randomized and was not done blindly, but experiments were repeated over a long study period (>2 years). Data analyses were done by a blinded investigator, and the conditions of the experiments were revealed only after all data were analyzed. No animals were excluded from the study. As indicated in Supplementary Fig.3, 7 young and 6 old slices representing 16% and 12% respectively of the total number of slices in each group, all originating from different animals, showed no LTP and hence were excluded from further LTP analyses. Statistical tests (one-way and two-way ANOVA, two-tailed paired or unpaired t-tests with uneaqual variances and sample sizes, two-tailed χ^2 tests, and nonparametric tests) and the exact p-values are clearly indicated in the text, figure legends, tables, and checklist. Significance was set at $p<0.05$. The distribution of individual data points is shown in most figures. In general, data distribution was assumed to be normal but this was not formally tested.

Data Availability

The data that support the findings including original films of the Western blots of this study are available from the corresponding author upon request.

Supplementary Material

Refer to Web version on PubMed Central for supplementary material.

Acknowledgments

This research was supported by a NIH-NINDS grant NS030549 (I.M.) and the Coelho Endowment to I.M. Confocal laser scanning microscopy was performed at the CNSI Advanced Light Microscopy/Spectroscopy shared resource facility at UCLA, supported with funding from NIH- NCRR shared resources grant (CJX1-443835-WS-29646) and NSF Major Research Instrumentation grant (CHE-0722519). We would like to thank W. Wei for performing the whole-cell recordings, Albert M. Barth for help with Igor procedures, Laurel Ormiston and R. Main Lazaro for expert technical assistance, and all members of the ModyLab for helpful comments during data presentation sessions.

References

1. Morrison JH, Baxter MG. The ageing cortical synapse: hallmarks and implications for cognitive decline. Nature Rev Neurosci. 2012; 13:240–250. [PubMed: 22395804]
2. Rosenzweig ES, Barnes CA. Impact of aging on hippocampal function: plasticity, network dynamics, and cognition. Progr Neurobiol. 2003; 69:143–179.
3. Malenka RC, Bear MF. LTP and LTD: an embarrassment of riches. Neuron. 2004; 44:5–21. [PubMed: 15450156]

4. Kastellakis G, Cai DJ, Mednick SC, Silva AJ, Poirazi P. Synaptic clustering within dendrites: an emerging theory of memory formation. Progr Neurobiol. 2015; 126:19–35.
5. Cox KJ, Adams PR. Hebbian crosstalk prevents nonlinear unsupervised learning. Front Comput Neurosci. 2009; 3:11. [PubMed: 19826612]
6. Cheng YF, et al. Curcumin rescues aging-related loss of hippocampal synapse input specificity of long term potentiation in mice. Neurochem Res. 2013; 38:98–107. [PubMed: 23011209]
7. Ris L, Godaux E. Synapse specificity of long-term potentiation breaks down with aging. Learning & Memory. 2007; 14:185–189. [PubMed: 17351142]
8. Larson J, Munkacsy E. Theta-burst LTP. Brain Res. 2015; 1621:38–50. [PubMed: 25452022]
9. Larson J, Lynch G, Games D, Seubert P. Alterations in synaptic transmission and long-term potentiation in hippocampal slices from young and aged PDAPP mice. Brain Res. 1999; 840:23–35. [PubMed: 10517949]
10. Megias M, Emri Z, Freund TF, Gulyas AI. Total number and distribution of inhibitory and excitatory synapses on hippocampal CA1 pyramidal cells. Neuroscience. 2001; 102:527–540. [PubMed: 11226691]
11. Higley MJ. Localized GABAergic inhibition of dendritic Ca(2+) signalling. Nature Rev Neurosci. 2014; 15:567–572. [PubMed: 25116141]
12. Wigström H, Gustafsson B. Facilitated induction of hippocampal long-lasting potentiation during blockade of inhibition. Nature. 1983; 301:603–604. [PubMed: 6298626]
13. Gagnon M, et al. Chloride extrusion enhancers as novel therapeutics for neurological diseases. Nature Med. 2013; 19:1524–1528. [PubMed: 24097188]
14. Kaila K, Price TJ, Payne JA, Puskarjov M, Voipio J. Cation-chloride cotransporters in neuronal development, plasticity and disease. Nature Rev Neurosci. 2014; 15:637–654. [PubMed: 25234263]
15. Medina I, et al. Current view on the functional regulation of the neuronal K^+-Cl^- cotransporter KCC2. Front Cell Neurosci. 2014; 8:27. [PubMed: 24567703]
16. Raimondo JV, Kay L, Ellender TJ, Akerman CJ. Optogenetic silencing strategies differ in their effects on inhibitory synaptic transmission. Nature Neurosci. 2012; 15:1102–1104. [PubMed: 22729174]
17. Andrásfalvy BK, Mody I. Differences between the scaling of miniature IPSCs and EPSCs recorded in the dendrites of CA1 mouse pyramidal neurons. J Physiol. 2006; 576:191–196. [PubMed: 16887875]
18. Doyon N, et al. Efficacy of synaptic inhibition depends on multiple, dynamically interacting mechanisms implicated in chloride homeostasis. PLoS Comput Biol. 2011; 7:e1002149. [PubMed: 21931544]
19. Mohapatra N, et al. Spines slow down dendritic chloride diffusion and affect short-term ionic plasticity of GABAergic inhibition. Sci Rep. 2016; 6:23196. [PubMed: 26987404]
20. Arosio D, Ratto GM. Twenty years of fluorescence imaging of intracellular chloride. Front Cell Neurosci. 2014; 8:258. [PubMed: 25221475]
21. Bakker A, et al. Reduction of hippocampal hyperactivity improves cognition in amnestic mild cognitive impairment. Neuron. 2012; 74:467–474. [PubMed: 22578498]
22. Koh MT, Haberman RP, Foti S, McCown TJ, Gallagher M. Treatment strategies targeting excess hippocampal activity benefit aged rats with cognitive impairment. Neuropsychopharmacol. 2010; 35:1016–1025.
23. Ferando I, Mody I. Front Neural Circ. 2013; 7:144.
24. Sarkar J, Wakefield S, MacKenzie G, Moss SJ, Maguire J. J Neurosci. 2011; 31:18198–18210. [PubMed: 22171026]
25. Ferando I, Mody I. Neuropharmacology. 2015; 88:91–98. [PubMed: 25261782]
26. Preibisch S, Saalfeld S, Tomancak P. Bioinformatics. 2009; 25:1463–1465. [PubMed: 19346324]

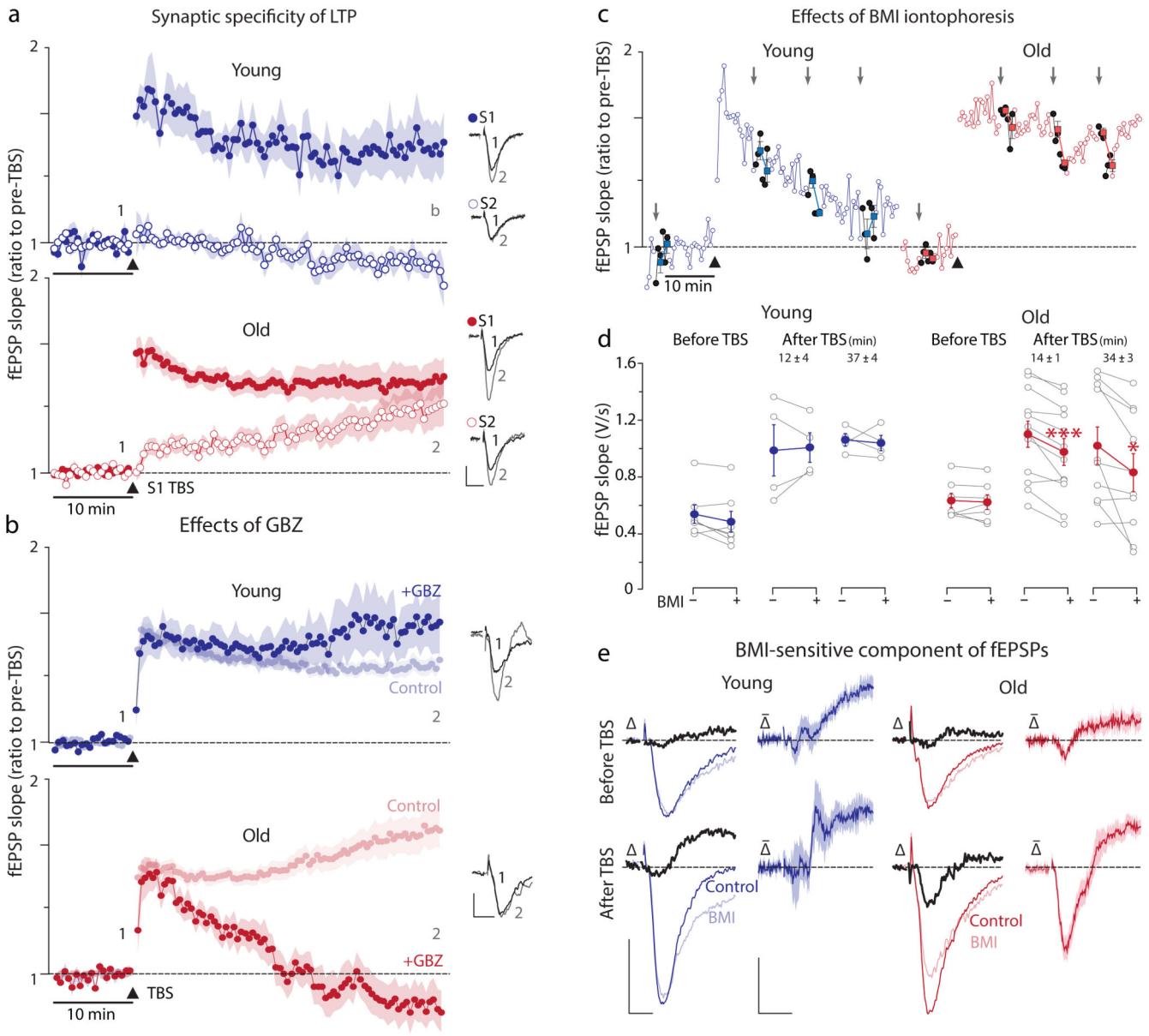

Fig.1.

Loss TBS-induced LTP synaptic specificity in old and the effects of blocking $GABA_A$ receptors on the induction and maintenance of LTP. (**a**) In young (*top panel*) TBS produces robust LTP in the tetanized pathway but not in the untetanized pathway. In old (*bottom panel*), LTP of S1 was similar to young, but the untetanized pathway was markedly potentiated compared to young (see Supplementary Table1 for details). Insets show example traces from the time points marked by "1" and "2". Calibrations apply to both panels: 1mV, 10ms. (**b**) In young GBZ (25μM) modestly increases the magnitude of LTP (1.84±0.20, n=11) but not significantly different (p=0.42, t=0.835, df=12.54, unpaired two-tailed t-test) from no GBZ controls (1.67±0.07, n=37). In sharp contrast, LTP induction is blocked by GBZ in old, as its magnitude at 40 min after TBS (fEPSP slope of pre-TBS values 0.73±0.16, n=11) is significantly lower than the 2.23±0.16 observed in the absence of any

drug (n=44; p=2.7e-7, t=6.48, df=32.45, unpaired two-tailed t-test). Calibrations apply to both panels: 0.5mV, 5ms. (**c**) Iontophoresis of BMI (*grey arrows*) into the str. radiatum in the close proximity of the recording electrode has little effect on fEPSPs recorded in young slices regardless of the timing before or after the TBS. In sharp contrast, BMI iontophoresis reduces fEPSPs in old slices, specifically after TBS. (**d**) Plot of all data points before (BMI -) and after (BMI +) iontophoresis showing that in old BMI significantly decreased fEPSP slopes both early and late after TBS (Supplemetary Table2) indicating the presence of a $GABA_A$ receptor-mediated component. (**e**) This component could be revealed by subtracting the fEPSPs immediately following BMI application from the traces preceding iontophoresis. The difference traces (Δ, *in black*) are fEPSP components blocked by BMI, i.e., mediated by $GABA_A$ receptors. The averaged difference traces ($\bar{\Delta}$) show no BMI-sensitive component in the young, but a dendritic negative-going (depolarizing) component in old (shaded = ±SEM). The subtracted negative going, and therefore depolarizing, $GABA_A$ receptor mediated (i.e., blocked by BMI) fEPSPs had an average 10-90% rise time of 1.67±0.13ms (n=12), not different from the rise times of fEPSPs mediated exclusively by ionotropic glutamate receptors (i.e., those in the presence of BMI) of 1.62±0.10ms (n=12, p=0.72, t=0.364, df=20.7, two-tailed unpaired t-test). Calibrations: 0.5mV, 5ms and 0.2mV, 5ms.

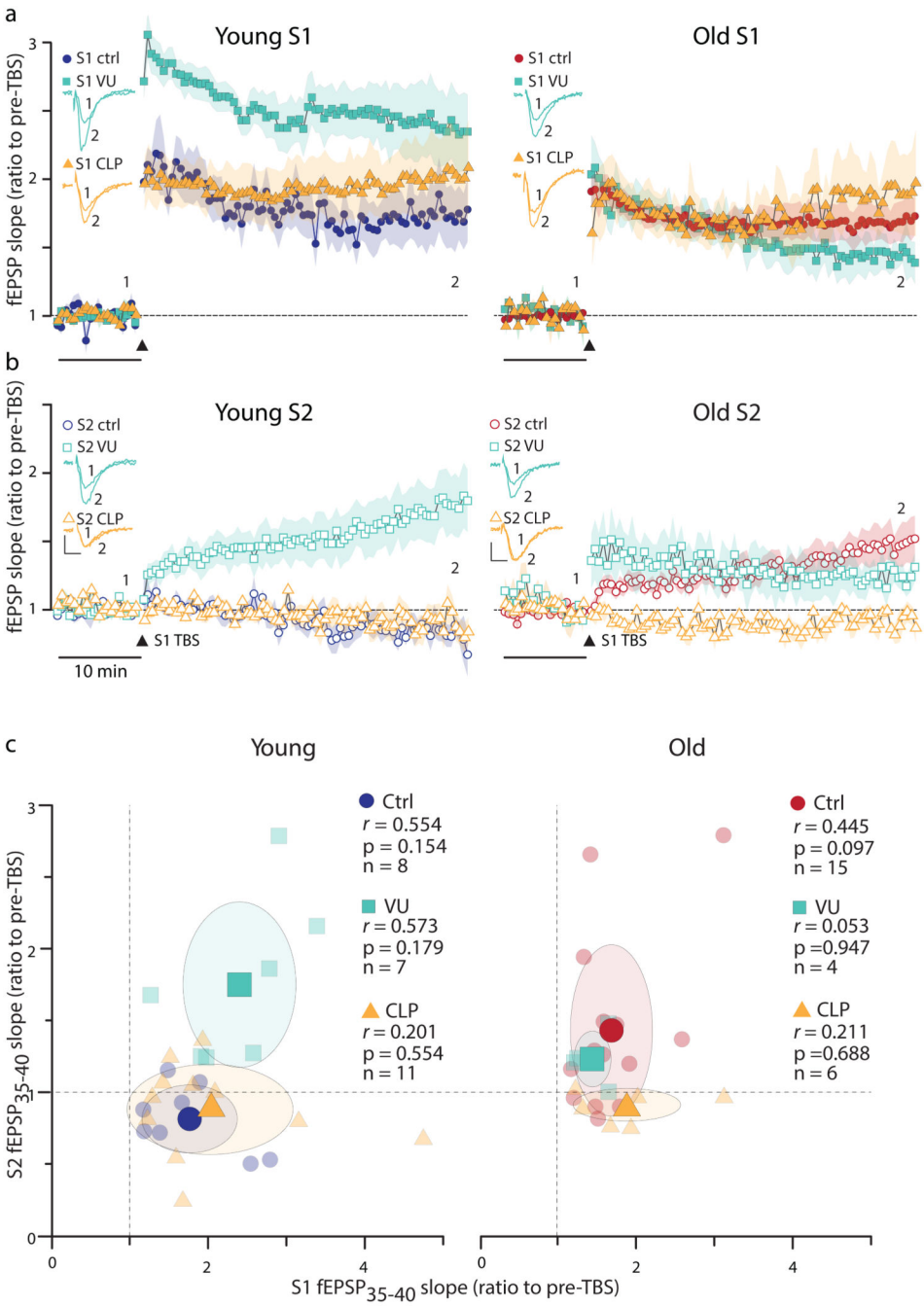

Fig. 2.

Effects KCC2 blockers and enhancers on LTP and its synapse specificity in young and old slices (also see Supplemetary Table3). Preincubation of young (n=7) with the KCC2 blocker VU0240551 (10μM, for 1hr) only slightly affected LTP (**a**) but spread the potentiation to untetanized synapses (**b**). Preincubation of young (n=11) with the KCC2 enhancer CLP-257 (100μM, for 1hr) did not affect the tetanized (S1) (**a**) or untetanized (S2) (**b**) responses. Enhancing KCC2 activity with CLP-257 (100μM, for 1hr) in old (n=6) did not affect LTP magnitude in the tetanized pathway (S1) (**a**), but significantly stopped the spread of

potentiation to untetanized synapses (**b**). Blocking KCC2 in old slices (n=4) with VU0240551 (10μM, for 1hr) did not change LTP of S1 (**a**) or its spread to S2 (**b**). Insets show example traces from the time points marked by "1" and "2". Calibration bars 0.5mV, 5ms. (**c**) Lack of correlation between the magnitude of LTP of the tetanized pathway (S1) and that of the untetanized pathway (S2). The average potentiation of the fEPSP slopes during 35-40 min after TBS ($fEPSP_{35\text{-}40}$) of the untetanized (S2) responses are plotted against the tetanized (S1) responses in young and old slices under three different conditions (Ctrl: control, VU:10 μM VU0240551, and CLP: 100μM CLP257). Legends indicate Pearson's correlation coefficients *r* and their p values according to a two-tailed t-test. Large symbols represent means of the x-y data and the shaded ovals are drawn at 1 × S.D. levels. The dotted lines at x=1 and y=1 indicate no potentiation. Symbols to the right of the x=1 line indicate LTP of S1, above the y=1 line indicate LTP of S2, and those above both lines show LTP of both S1 and S2.

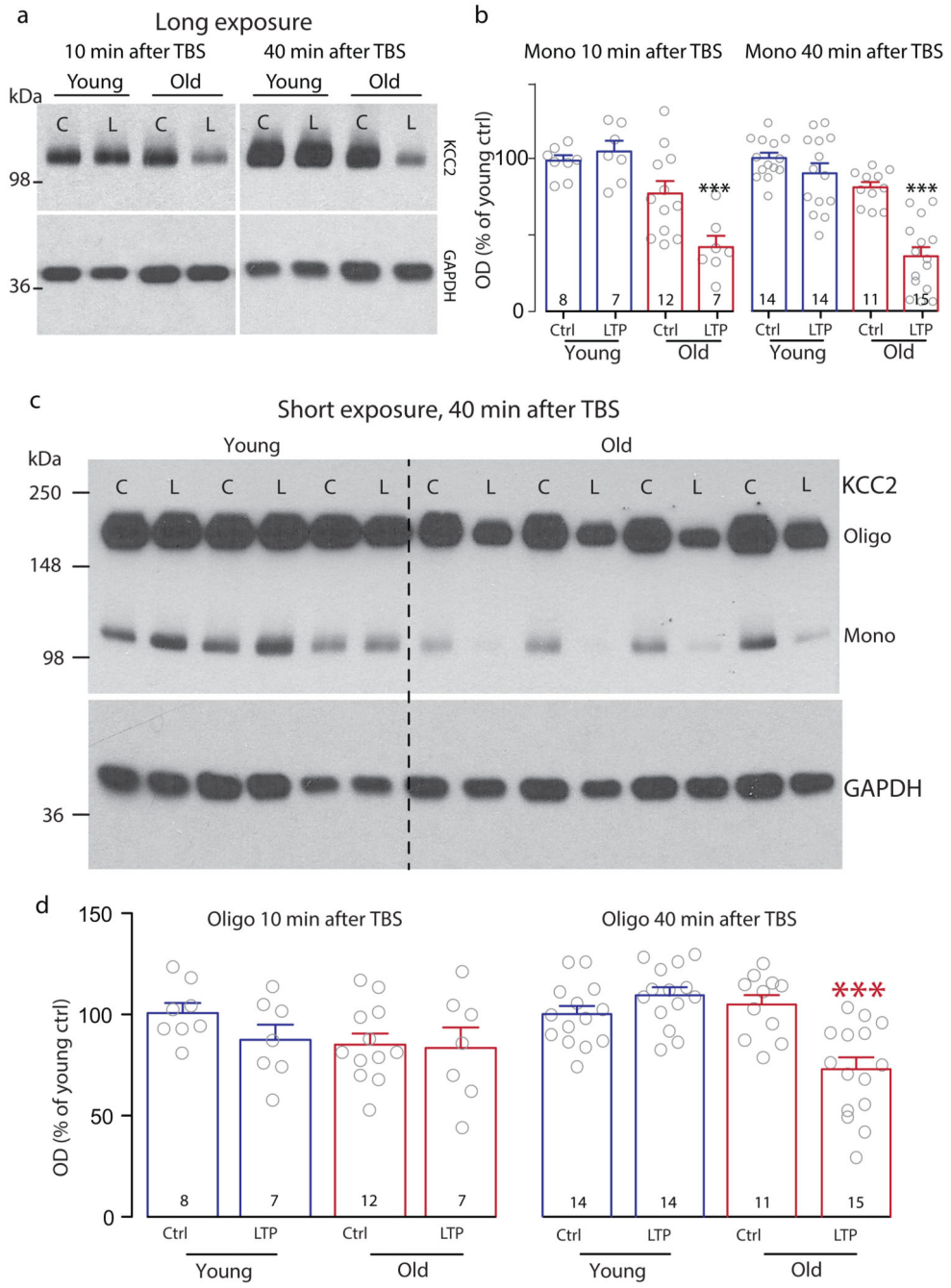

Fig. 3.

Quantitative analyses of Western blots of monomeric and oligomeric KCC2 levels. (**a**) Representative Western blots of monomeric KCC2 and loading controls (GAPDH) from two minislices each from young and old, harvested after recordings before (“C”), or 10 min or 40 min after the LTP-inducing TBS (“L”). (**b**) Summary data showing reduced monomeric KCC2 levels in old slices at 10 min and 40 min after TBS. Values were normalized to the average of the young unstimulated controls (“Ctrl”). Post-one-way ANOVA (10 min post-TBS $F[3, 30] = 12.34$, $p<0.0001$ and 40 min post-TBS $F[3, 50] = 31.75$, $p<0.0001$) multiple

comparisons with Tukey's correction indicate at each time point the “old LTP” groups are significantly different from every other group (at 10 min: old LTP vs young control p= 0.0001, vs young LTP p<0.0001, vs old control p=0.0092; at 40 min: old LTP vs every other group p<0.0001). (**c**) Full-length blots of protein samples as in (a), but exposure time was shortened for visualizing the higher molecular weight oligomeric KCC2. (**d**) Summary data as in (b) for oligomerized KCC2. One-way ANOVA shows a significant difference between the groups at 40 min, but not at 10 min, after TBS (10 min: $F[3, 30] = 1.253$, $p=0.3080$; 40 min: $F[3, 50] = 12.39$, $p<0.0001$). At 40 min after TBS, the “old LTP” is significantly lower than every other group (vs young control p= 0.0008, vs young LTP p<0.0001, vs old control p=0.0002, Tukey's correction for multiple comparisons).